

Oxygen-Coverage Effects on Molecular Dissociations at a Pt Metal Surface

R. B. Getman,¹ W. F. Schneider,^{1,2,*} A. D. Smeltz,³ W. N. Delgass,³ and F. H. Ribeiro^{3,†}

¹Department of Chemical and Biomolecular Engineering, University of Notre Dame, Notre Dame, Indiana 46556, USA

²Department of Chemistry and Biochemistry, University of Notre Dame, Notre Dame, Indiana 46556, USA

³School of Chemical Engineering, Purdue University, West Lafayette, Indiana 47907, USA

(Received 2 June 2008; published 17 February 2009)

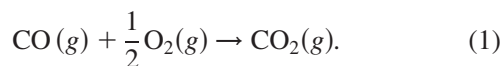
The effects of adsorbate coverage on catalytic surface reactions are not well understood. Here, we contrast the rates of O₂ and NO₂ dissociations, two competing reactions in NO oxidation catalysis, versus oxygen coverage at a Pt(111) surface. *In situ* x-ray photoelectron spectroscopy experiments show that the NO₂ dissociation rate is less sensitive to O coverage than is O₂. Density-functional theory simulations reveal an NO₂ reaction pathway that is more adaptable to an increasingly crowded surface than is O₂ dissociation. While the rates are comparable at low coverage, NO₂ dissociation is many orders of magnitude faster at O coverages typical of NO oxidation catalysis.

DOI: 10.1103/PhysRevLett.102.076101

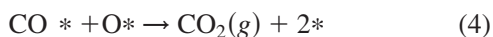
PACS numbers: 82.65.+r, 68.35.Md, 68.43.Bc

Catalytic oxidations with O₂ are common in exhaust gas aftertreatment, in chemical processing, and even in extraction of energy from fuel. The late transition metals are common catalysts, and the intrinsic activities of these materials are often observed to depend sensitively on reaction conditions [1–3]. This sensitivity is now recognized to arise from changes in surface adsorbate coverage and near-surface composition [4–7], that appear under catalytic conditions.

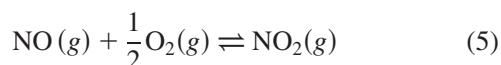
CO oxidation to CO₂ over Pt offers one illustration of coverage-dependent reactivity [4]:



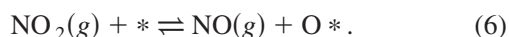
The reaction is well described by a Langmuir-Hinshelwood model [4,8]:



and observed reaction rates and orders depend on whether the metal surface is O or CO covered [1,3]. Isostoichiometric NO oxidation is also Pt catalyzed [9,10],



and might be expected to exhibit similar behavior. However, (5) is much less exothermic than (1) (−57 vs −283 kJ mol^{−1}) and must be catalyzed at high P_{O₂} (≈0.1 atm) and modest T to drive the equilibrium towards products. Further, unlike CO₂, NO₂ is an effective O atom donor to Pt [11].



Oxygen is thus expected to dominate the Pt catalyst surface, and high O coverages have been proposed and observed to account for NO oxidation activity [9,10,12,13]. Chemisorbed O interacts repulsively at Pt surfaces [14–16], and the weakening of the Pt–O bond with increasing O coverage drives the formation of NO₂. A successful model of NO oxidation thus must capture both realistic surface O coverage and its effects on the energetics and kinetics of surface reactions.

In this Letter, we report *in situ* x-ray photoelectron spectroscopy (XPS) experiments and density-functional-theory (DFT) calculations to establish the O coverage, θ_O, and to contrast the rates of O₂ and NO₂ dissociations at realistic NO oxidation conditions over Pt. We demonstrate that: (1) θ_O can exceed 0.6 monolayer (1 ML ⇒ O/Pt = 1); (2) under thermodynamically identical conditions, NO₂ dissociates more readily than does O₂; and (3) the kinetic advantages of NO₂ at increasing coverage reflect a dissociation pathway that is more adaptable to an increasingly crowded Pt surface. Surface coverage has been shown to differently affect NO and O₂ dissociation rates on Ni(100) at ultrahigh vacuum conditions [17]; the results here provide direct evidence for different O atom addition rates at near-ambient pressures relevant to catalysis.

Initial flow reactor experiments were performed to determine the NO oxidation activity of Pt particles supported on alumina [9,10]. A positive correlation between turnover rate (TOR) and particle size strongly implicates the close-packed Pt surface as the locus of highest activity. Experiments with a Pt(111) single crystal confirm the high TOR on this crystal face [13], and we focus further work on this surface.

In situ XPS experiments were performed at Beamline 9.3.2.1 at the Advanced Light Source, LBL to determine the amount and chemical identity of Pt-bound O arising from exposure to reactive gases. This system allows XP spectra to be taken at temperatures and pressures up

to 775 K and 5 Torr [18], allowing us to probe Pt-bound species near reaction conditions. This technique uniquely gives direct, quantitative, surface sensitive chemical information at reaction conditions relevant to NO oxidation. Prior to each experiment, the Pt(111) single crystal was sputter cleaned and annealed at 975 K for 10 minutes. This procedure yielded a clear (111) LEED pattern in separate experiments. No impurities were detected after annealing and during the experiments except for a trace amount of iodine, maximum coverage estimated to be <0.05 ML, present during experiments with NO due to reaction with contaminated walls of the vacuum chamber. The incident photon energy was set to 825 eV for the $\text{Pt}_{4p_{3/2}}/\text{O}_{1s}$ region to maximize surface sensitivity while avoiding significant spectrometer inefficiencies at low kinetic energies. The binding energy scale was calibrated to the $\text{Pt}_{4f_{7/2}}$ transition at 70.9 eV, which was measured each time the incident photon energy or conditions were adjusted.

Two conditions were used to build a linear O coverage calibration between 0–3/4 ML. First, the Pt(111) single crystal was saturated using 10^{-5} Torr O_2 at 380 K, conditions that are well known to produce the 1/4 ML $p(2 \times 2)$ -O pattern [16]. The second calibration point was saturation NO_2 exposure at 10^{-6} Torr and 450 K, which yields 3/4 ML O and no adsorbed NO [11]. The $\text{Pt}_{4p_{3/2}}/\text{O}_{1s}$ intensity ratios were determined at each condition. Five spectra were taken over a period of 90 minutes for each calibration point to verify that a steady surface coverage had been obtained and for statistics.

To determine the maximum coverage θ_{O} from O_2 dosing, the Pt(111) sample was exposed to 0.1 Torr O_2 , the temperature incrementally increased from 353 to 663 K, and spectra collected at various intermediate points (Table I). Each T change took 10–15 minutes and was followed by 30–45 minutes of spectra collection. The data at 518 K were taken independently and started with a clean Pt surface. The error bar represents the standard deviation from five measurements of the $\text{Pt}_{4p_{3/2}}/\text{O}_{1s}$ region. No significant change in O coverage was observed during the 1 h of spectra collection at each condition. Previous UHV experiments have only been able to achieve θ_{O} greater than 1/4 ML with extraordinary methods. The higher pressure of 0.1 Torr used here generated θ_{O} up to 0.54 ± 0.04 ML. This coverage is seemingly the maximum kinetically accessible by O_2 dissociation at this moderate pressure, similar to that found over Ru(0001) [19].

Low-pressure ($\approx 10^{-6}$ Torr) NO_2 dosing at 450 K is documented to produce 3/4 ML O [11] on Pt(111). Our *in situ* XPS experiments show that increasing P_{NO_2} to

0.2 Torr at 450 K as well as a subsequent increase in temperature to 520 K have no significant effect on the measured value θ_{O} . No high binding energy shoulder on the Pt_{4f} doublet or a second O_{1s} peak due to PtO_x formation was observed. No N_{1s} transition peak was found, indicating negligible amounts of surface-bound NO and N and implying that O was the most prevalent surface species.

Similar pressures of O_2 and NO_2 thus generate significant yet different O coverages on Pt(111), a result that could be attributable to the differing thermodynamics and/or kinetics of O deposition by these two oxidants. To test this question, we compared measured θ_{O} resulting from O_2 and NO_2 dosing under conditions at which each would produce identical coverages if equilibrium between gas-phase and surface oxygen is attained [15]. We assume that NO_2 and O_2 add O to Pt(111) according to reactions (6) and (3), respectively, and select dosing conditions corresponding to equilibrium between gas-phase NO, O_2 , and NO_2 , that is, conditions at which $1/2\mu_{\text{O}_2} = \mu_{\text{NO}_2} - \mu_{\text{NO}}$ [15].

We carried out experiments at 518 K and used a mixture of 0.1, 0.05, and 0.05 Torr of O_2 , NO, and NO_2 , respectively, that is at chemical equilibrium at this temperature (Table II). Exposure to 0.05 Torr NO and 0.05 Torr NO_2 yields $\theta_{\text{O}} = 0.63 \pm 0.04$ ML, 0.1 ML greater than the coverage achieved with O_2 . Addition of 0.1 Torr O_2 to this NO_x mixture changes θ_{O} negligibly, to 0.62 ± 0.03 ML. Based on the 95% confidence limits from a one-sided t -test assuming unequal variances, θ_{O} from the NO_2/NO mixture was greater than that from 0.1 Torr O_2 alone despite the equal chemical potentials of the two O sources. Thus, the higher coverages from NO_2 exposure reflects an advantage in the *kinetics* of NO_2 dissociation over O_2 . These gas concentrations are representative of NO oxidation catalysis at high conversion. The results indicate that over Pt(111) [13], the O coverage is 0.63 ± 0.04 ML, that this coverage arises from the favorable kinetics of NO_2 dissociation relative to O_2 , and support the proposal that the NO_2/NO reaction controls O coverage during NO oxidation over Pt.

To understand this difference in dissociation rates, we used supercell DFT calculations to contrast the O_2 and NO_2 dissociations on Pt(111) as a function of O coverage. Based on previous DFT determination of the coverage dependence of O binding energies [15] and consistent with experimental characterization of chemisorbed oxygen

TABLE I. Oxygen coverages on Pt(111) measured by *in situ* XPS from exposure to 0.1 Torr O_2 (g) at various T . The measurement error is ± 0.05 ML unless indicated.

T (K)	353	433	488	518	593	663
θ (ML)	0.48	0.49	0.52	0.54 ± 0.04	0.40	0.39

TABLE II. Observed O coverage on Pt(111) at 518 K from different gas mixtures at identical O chemical potentials. Pressures in Torr.

P_{O_2}	0.1	0	0.1	0
P_{NO_2}	0	0.05	0.05	10^{-6}
P_{NO}	0	0.05	0.05	0
θ (ML)	0.54 ± 0.04	0.63 ± 0.04	0.62 ± 0.03	0.75

structures up to 1/2 ML O [20], we chose 4-layer thick, 4×4 supercells of clean Pt(111), 1/4 ML $p(2 \times 2)$ -O, and 1/2 ML $p(2 \times 1)$ -O as O coverage models [15,20]. The minimum energy paths [21] for O_2 and NO_2 dissociation were determined in each model (Figs. 1 and 2).

O_2 adsorbed in a bridge site on clean Pt(111) (Fig. 1, R) dissociates along a path in which the molecule stretches and slides sideways into neighbor fcc sites [24]. O_2 span bridge and top sites and are separated by 1.88 Å at the transition state (TS) (Fig. 1, S). The low-coverage TS is calculated to be 0.24 eV below the energy of separated Pt(111) and $O_2(g)$, about 0.2 eV less than molecular beam and TPD experiments [16]. At higher O coverage, repulsive adsorbate-adsorbate interactions distort the initial and transition states. We compute the energy penalty for O and O_2 to share a surface Pt atom to be 0.36 eV ($d_{O-O_2} \approx 2.9$ Å), or about twice the penalty for two O to be nearest neighbors [15]. To reduce these interactions, adsorbed O_2 adopts a “near top-bridge-near top” twisted geometry (Fig. 1, M). In the $p(2 \times 2)$ -O and $p(2 \times 1)$ -O models, adsorbed O_2 suffers one and three of these nearest-neighbor interactions, respectively, enough to make adsorption approximately thermoneutral in the former case and endothermic in the latter. At these higher coverages,

O_2 dissociation occurs by rotation about a surface normal and stretching of the O–O bond until the O occupy adjacent fcc sites. The O–O distances at the transition states increase to 1.60 and 1.76 Å on $p(2 \times 2)$ -O and $p(2 \times 1)$ -O, respectively. The TS interacts with two and six neighbor O (Fig. 1, P), increasing the energy barriers to 1.0 and 2.3 eV above $O_2(g)$.

These results are consistent with a dramatic decrease in O_2 dissociation rate with increasing O coverage. To circumvent errors in the absolute DFT barriers, we calculate relative dissociation rates with respect to the clean Pt(111) surface according to

$$\frac{r(\theta_O)}{r(\theta_O = 0)} = \frac{Q_{\text{vib}}^\ddagger(\theta_O)}{Q_{\text{vib}}^\ddagger(\theta_O = 0)} \times \exp\left[-\frac{E^\ddagger(\theta_O) - E^\ddagger(\theta_O = 0)}{k_B T}\right]. \quad (7)$$

At 518 K and 0.1 Torr O_2 , the experimental conditions considered above, the O_2 dissociation rates decrease to 3×10^{-12} and 6×10^{-24} that of the clean surface, respectively.

NO_2 can adsorb in several orientations on clean Pt(111) [12,23]. The μ -N,O-nitrito configuration, in which bent NO_2 binds with one bond parallel to the metal surface, is lowest in energy (Fig. 2, X), and dissociation from this configuration occurs by migration of O and NO to adjacent fcc sites [12]. The TS is 0.35 eV below the $NO_2(g)$ entrance channel, and based on the relative energies and partition functions at the TS relative to the respective gases, we estimate the NO_2 dissociation rate to be 88 times that of O_2 at 518 K and $P_{O_2}/P_{NO_2} = 2$.

The energy penalty for NO_2 to share a surface Pt with chemisorbed O is 0.38 eV, nearly identical to that for O_2 . However, the coordinative flexibility of NO_2 allows it to more easily adapt to higher O coverage, moving from an O, N-down configuration to one that makes a single bond with Pt. We construct a minimum energy pathway starting from an O-down atop Pt configuration (Fig. 2, U) that has zero and one nearest-neighbor O on $p(2 \times 2)$ -O and $p(2 \times 1)$ -O, respectively. Nudged elastic band calculations identify a pathway in which O shifts to an adjacent fcc site and product NO moves atop Pt to decrease interactions with chemisorbed O. Consistent with atop NO binding [23], the off-surface O–N bond is shorter in the TS and product than at low coverage. In the reactant, the on-surface O–N distance is notably larger, indicating bound NO_2 is more readily dissociable at high coverage. The dissociation barrier with respect to $NO_2(g)$ increases with increasing O coverage, consistent with a decrease in product binding energies, but the effects are moderated by the changes in reactant, TS, and product configurations that reduce adsorbate-O interactions. The calculated NO_2 dissociation rate does decrease with O coverage, to 10^{-4} and 10^{-11} that on clean Pt(111) at $p(2 \times 2)$ -O and $p(2 \times 1)$ -O, respectively, but this decrease is not nearly as drastic as for O_2 . At the highest O coverage, we estimate the rate of NO_2

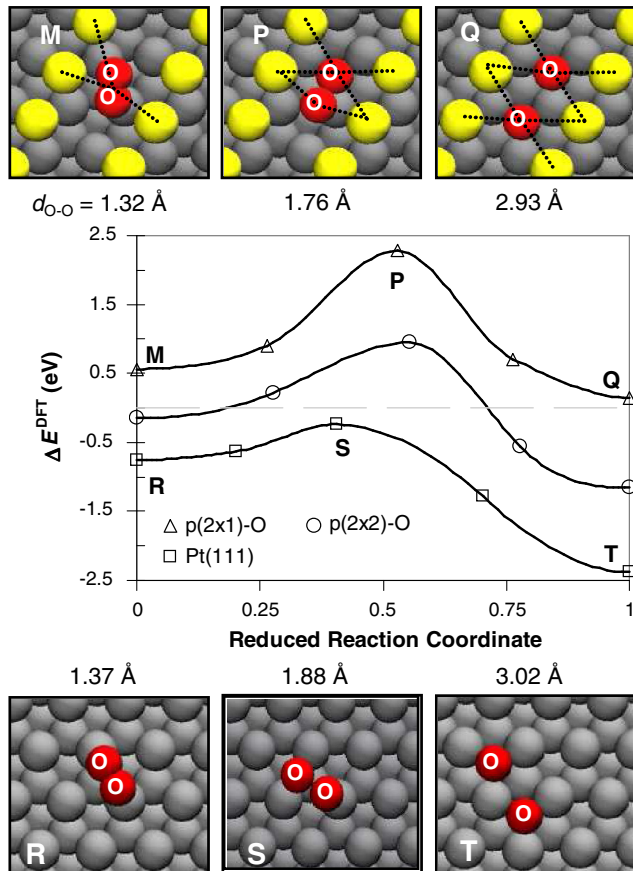


FIG. 1 (color online). Minimum energy paths referenced to $O_2(g)$ and geometries for $O_2^* \rightarrow 2O^*$. Dotted lines label 1st nearest-neighbor interactions.

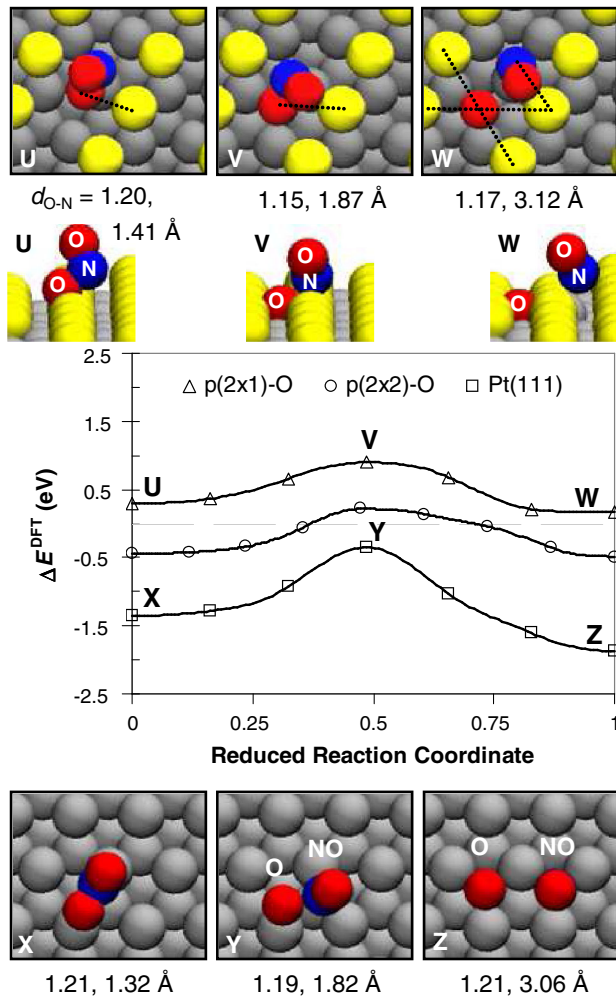


FIG. 2 (color online). Minimum energy paths referenced to $\text{NO}_2(g)$ and geometries for $\text{NO}_2^* \rightarrow \text{NO}^* + \text{O}^*$. Dotted lines label 1st nearest-neighbor interactions.

dissociation to be 10^{12} times that of O_2 at $P_{\text{NO}_2}/P_{\text{O}_2} = 1/2$.

The DFT results demonstrate, consistent with experiment, the kinetic advantages of NO_2 over O_2 in developing high O coverages on Pt(111). In principle, the θ_{O} can attain values above those at which surface oxygen is energetically unstable to associative desorption of O_2 : as shown in Fig. 1, O_2 desorption remains a highly activated process even at high O coverages. This metastability likely contributes to the explosive desorption of O_2 observed from Pt surfaces dosed with atomic O [25].

In summary, we report experiments and DFT simulations to characterize a Pt surface at conditions representative of NO oxidation catalysis. We show that the metal surface attains coverages greater than 0.6 ML O, and that while O_2 dissociation slows drastically with increasing O coverage, NO_2 dissociation remains facile due to greater coordinative flexibility in the dissociation pathway. The results indicate an NO oxidation mechanism quite different

from CO oxidation, in which product NO_2 inhibits the forward rate by driving high surface O coverages, and O_2 reactions are rate limiting [9,10,13].

Support from the Department of Energy Basic Energy Sciences under Grants No. DE-FG02-06ER15839 and No. DE-FG02-03ER15408 as well as computer time at the Northwest Indiana Computational Grid are gratefully acknowledged. The authors thank R. M. Rioux, B. Kromer, B. R. Fingland, W. S. Epling, B. S. Mun, and D. Zemlyanov for their helpful assistance and Ye Xu for his insights.

*wschneider@nd.edu

†fabio@purdue.edu

- [1] G. Ertl, *Science* **254**, 1750 (1991).
- [2] C. Peden and D. W. Goodman, *J. Phys. Chem.* **90**, 1360 (1986).
- [3] M. S. Chen *et al.*, *Surf. Sci.* **601**, 5326 (2007).
- [4] G. Ertl, *Angew. Chem., Int. Ed.* **47**, 3524 (2008).
- [5] H. Over *et al.*, *Science* **287**, 1474 (2000).
- [6] M. Tadorova *et al.*, *Phys. Rev. Lett.* **89**, 096103 (2002).
- [7] G. Ertl, *Angew. Chem., Int. Ed.* **29**, 1219 (1990).
- [8] C. T. Campbell, G. Ertl, H. Kuipers, and J. Segner, *J. Chem. Phys.* **73**, 5862 (1980).
- [9] S. Mulla *et al.*, *Catal. Lett.* **100**, 267 (2005).
- [10] S. S. Mulla *et al.*, *J. Catal.* **241**, 389 (2006).
- [11] M. E. Bartram, B. E. Koel, and E. A. Carter, *Surf. Sci.* **219**, 467 (1989).
- [12] S. Ovesson, B. I. Lundqvist, W. F. Schneider, and A. Bogicevic, *Phys. Rev. B* **71**, 115406 (2005).
- [13] A. D. Smeltz, R. B. Getman, W. F. Schneider, and F. H. Ribeiro, *Catal. Today* **136**, 84 (2008).
- [14] Y. Y. Yeo, L. Vattuone, and D. A. King, *J. Chem. Phys.* **106**, 392 (1997).
- [15] R. B. Getman, Y. Xu, and W. F. Schneider, *J. Phys. Chem. C* **112**, 9559 (2008).
- [16] C. T. Campbell, G. Ertl, H. Kuipers, and J. Segner, *Surf. Sci.* **107**, 220 (1981).
- [17] L. Vattuone, Y. Y. Yeo, and D. A. King, *J. Chem. Phys.* **104**, 8096 (1996).
- [18] D. F. Ogletree *et al.*, *Rev. Sci. Instrum.* **73**, 3872 (2002).
- [19] C. Stampfl *et al.*, *Phys. Rev. Lett.* **77**, 3371 (1996).
- [20] S. P. Devarajan, J. A. Hinojosa Jr., and J. F. Weaver, *Surf. Sci.* **602**, 3116 (2008).
- [21] The climbing image nudged elastic band method [22] was used to locate minimum energy pathways. Initial images were constructed with one O_2 or NO_2 per supercell. Structures were separated by no more than 1 Å and relaxed to $0.05 \text{ eV } \text{Å}^{-1}$. Further details have been published previously [13,15,23].
- [22] G. Henkelman, B. P. Uberuaga, and H. Jonsson, *J. Chem. Phys.* **113**, 9901 (2000).
- [23] R. B. Getman and W. F. Schneider, *J. Phys. Chem. C* **111**, 389 (2007).
- [24] Ž. Šljivančanin and B. Hammer, *Surf. Sci.* **515**, 235 (2002).
- [25] J. F. Weaver, J.-J. Chen, and A. L. Gerrard, *Surf. Sci.* **592**, 83 (2005).